Available online at www.sciencedirect.com
SCIENCE DIRECT®
Pattern Recognition 38 (2005) 2132–2142
PATTERN RECOGNITION
THE JOURNAL OF THE PATTERN RECOGNITION SOCIETY
www.elsevier.com/locate/patcog

A content-based system for human identification based on bitewing dental X-ray images☆

Jindan Zhou, Mohamed Abdel-Mottaleb*

Department of Electrical and Computer Engineering, University of Miami, 1251 Memorial Drive, Coral Gables, FL 33146, USA

Received 14 September 2004; received in revised form 27 December 2004; accepted 4 January 2005

Abstract

This paper presents a system for assisting in human identification using dental radiographs. The goal of the system is to archive antemortem (AM) dental images and enable content-based retrieval of AM images that have similar teeth shapes to a given postmortem (PM) dental image. During archiving, the system classifies the dental images to bitewing, periapical, and panoramic views. It then segments the teeth and the bones in the bitewing images, separates each tooth into the crown and the root, and stores the contours of the teeth in the database. During retrieval, the proposed system retrieves from the AM database the images with the most similar teeth to the PM image based on Hausdorff distance measure between the teeth contours. Experiments on a small database show that our method is effective for dental image classification and teeth segmentation, provides good results for separating each tooth into crown and root, and provides a good tool for human identification.

Keywords: Biometrics; Dental images; Image segmentation; Human identification; Forensic odontology; Dental image classification

1. Introduction

Reliable identification of humans is important for many applications, such as law enforcement, border control, homeland security and airport security. Dental features are regarded as the best candidates for postmortem (PM) biometric identification. Not only they represent a suitable repository for unique and identifying features, but they also survive most PM events that can disrupt or change other body tissues, e.g. bodies of victims of violent crimes, motor vehicle accidents, and work place accidents, whose bodies can be disfigured to such an extent that identification by a family member is neither reliable nor desirable [1–3]. For these reasons, human identification based on dental features has always played a very important role in forensics.

There are two scenarios for the use of dental identification. In the first scenario, a comparative identification is used to establish the degree of certainty that the dental records obtained from the remains of a decedent and the antemortem (AM) dental records of a missing person are for the same individual. In the second scenario, the AM records are not available, and no clues to the possible identity exist. In this case, a PM dental profile is completed by the forensic odontologist suggesting characteristics of the individual in order to narrow down the search. Traditionally, this kind of identification work is carried manually by forensic odontologists [4].

Basically, comparative dental identification methods, in which PM dental records are analyzed and compared against AM records to confirm identity, relying on dental

☆ This research is supported in part by the US National Science Foundation under Award number EIA-0131079, the research is also supported under Award number 2001-RC-CX-K013 from the Office of Justice Programs, National Institute of Justice, US Department of Justice.

* Corresponding author. Tel.: +1 305 284 3825; fax: +1 305 284 4044.
E-mail addresses: jzhou@umsis.miami.edu (J. Zhou), mottaleb@miami.edu (M. Abdel-Mottaleb).

0031-3203/$30.00
doi:10.1016/j.patcog.2005.01.011

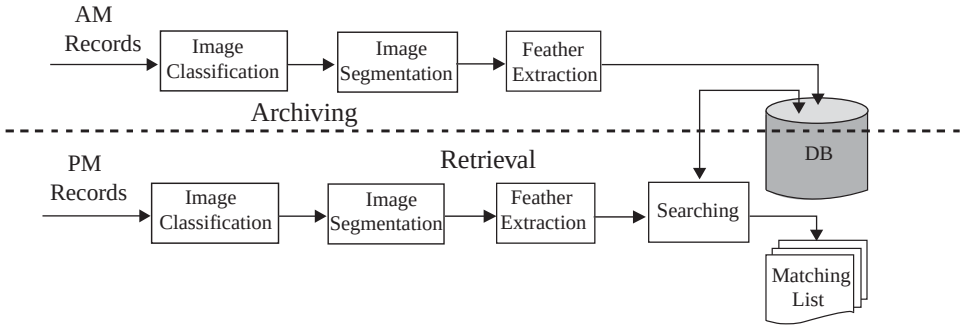

Fig. 1. Archiving and retrieval stages of human identification system.

restoration and dental work features rather than inherent tooth characteristics, e.g., morphology of teeth and roots. Clearly, individuals with numerous and complex dental treatments are often easier to identify than those individuals with little or no restorative treatment. But, in many cases these features are not enough to get correct identifications, moreover, these identification methods are not fully automated as image comparison is carried out manually [5–7]. In the future, these features may become unreliable and difficult to use due to the advances in dentistry. For example, contemporary generations have less dental decay than their predecessors; also cavities in today's children and their offsprings will be virtually undetectable because of using hi-tech pit and fissure sealants. Consequently, it becomes important to develop automatic dental identification systems using inherent dental features [8], such as shapes of roots and crowns, and space between teeth, for substituting the manual methods [9–11]. Recent special issues of the IEEE Computer and ACM Communications survey the state of the art in biometric identification technologies and discuss future trends [12,13].

To build automatic dental identification systems, there are several challenges. For example, dental features may change over time. Therefore, they are not always reliable and the system needs to decide when to rely on them and when to ignore them. Meanwhile, the system needs to handle dental radiographs of poor quality and take view variance of the images into consideration. An important issue is the segmentation of the teeth from the radiograph. This step is crucial for the success of the automated dental identification system, because the accuracy of the extracted features depends on the results of the segmentation.

Current research on automated dental identification systems focuses on shape features [14,15,27,28]. During archiving, they segment the AM images, extract and store either teeth contours or contour descriptors in a database. During retrieval, a PM image is submitted, and these systems segment the image and obtain contours of the teeth or contour descriptors, then match them with the ones in the AM database. The best matches are then presented to the user.

In this paper we present a system for archiving and retrieval of dental images to be used in identification based on dental images. The system includes steps for dental image classification, automatic segmentation of bitewing dental X-ray images, and teeth shape matching. The main reason for working with bitewing images is that the shapes of molar teeth in bitewing images are considered more distinctive than other teeth. Also, the bones are usually visible and distinguishable from the teeth and can be used to separate the roots from the crowns of the teeth. As we will see in the experiments, since the quality of bitewing images is usually not poor, most of the teeth in these images could be successfully separated into crowns and roots, which is potentially important for extracting features for identification.

The paper is organized as follows: Section 2 introduces our method for classifying the three types of dental images, details the algorithm for segmenting bitewing images, and describes the teeth matching algorithm. Section 3 discusses the experimental results of the classification, segmentation, and retrieval using the proposed methods in Section 2. The conclusions and the future work are discussed in Section 4.

2. System components

Fig. 1 shows a high-level diagram of our system. The system contains two stages: archiving and retrieval. During archiving, the system processes AM images, classifies and segments them, extracts the teeth contours and archives them in a database. In the retrieval stage, a PM image is submitted; the system classifies and segments the image and uses extracted contours of the teeth to calculate shape distance between the PM and the AM images, and presents AM images with the smallest distances to the user. The details of the system components: dental image classification, image segmentation, shape-based retrieval, are presented in the rest of this section.

2.1. Dental image classification

Image classification is the first step in the system. In our system, there are three types of dental images according to the way they capture the dental features, i.e., panoramic, periapical and bitewing (see Fig. 2). The periapical images are

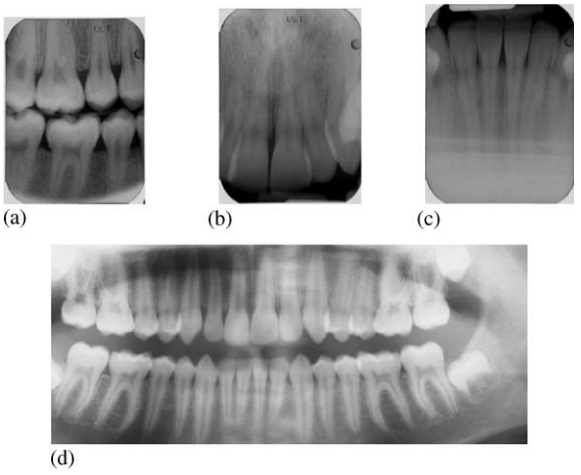

Fig. 2. The three types of dental images: (a) bitewing; (b) upper periapical; (c) lower periapical; (d) panoramic.

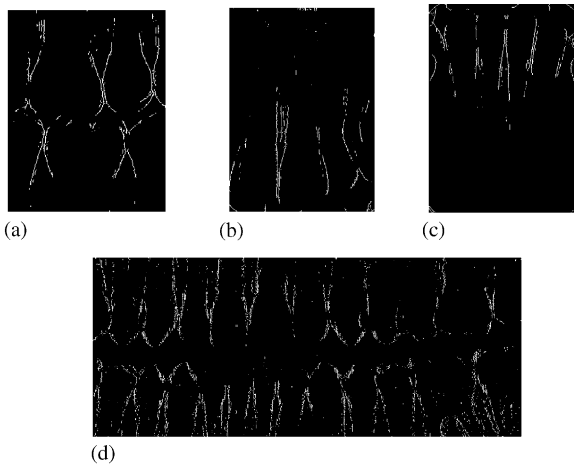

Fig. 3. Vertical edges in the three types of dental images: (a) bitewing; (b) upper periapical; (c) lower periapical; (d) panoramic.

further subclassified into upper periapical, which shows the upper jaw, and lower periapical, which shows the lower jaw. Different types of dental radiographs contain different information of dental features. Our system classifies the dental images and only archives the bitewing images. In the future, we plan to use the classification results to select the appropriate archiving procedure for each type of images.

Panoramic images show more teeth than perapical and bitewing images, and therefore have more vertical edges which correspond to the teeth's boundaries (see Fig. 3). We can use the number of vertical edge pixels as a feature to distinguish between the panoramic images and the other two types of dental images. In order to distinguish between periapical and bitewing images, we use a feature related

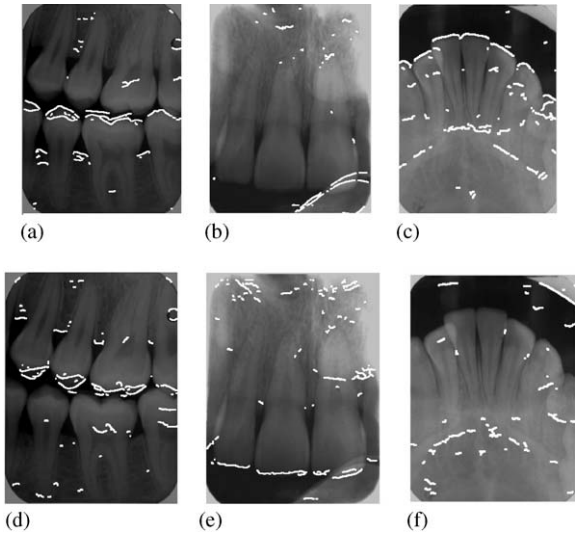

Fig. 4. Horizontal edges with upward gradient in (a) bitewing; (b) upper periapical; (c) lower periapical. Horizontal edges with downward gradient in (d) bitewing; (e) upper periapical; (f) lower periapical.

to the orientation of horizontal and near horizontal edges. There are two types of horizontal (or near horizontal) edges: one with upward gradient and the other with downward gradient. It is clear that a periapical image has more of one type of these edges than the other, while a bitewing image or a panoramic image has nearly equal horizontal (and near horizontal) edges with both upward and downward gradients (see Fig. 4). The second feature we use is either the ratio of the number of horizontal edges with upward gradient to the total number of horizontal edges, or the ratio of the number of horizontal edges with downward gradient to the total number of horizontal edges.

From the discussion above, we have a total of two features to classify the three types of images: (1) the number of vertical edge pixels in the image normalized by the number of rows in the image; and (2) ratio of horizontal edges with upward gradient to the total amount of horizontal edges. These two types of features are only related to the content of the dental images and are independent of the size of the image.

Given a dental image, a Bayes classifier is used to classify the dental image as follows: let c_i denotes the ith class, where $i = 1, 2, 3, 4$ for panoramic, bitewing, upper periapical or lower periapical class, respectively. According to the Bayes rule, the posteriori probability of an image with feature vector x being from class c_i is

$$p(c_i|x) = \frac{p(x|c_i)p(c_i)}{p(x)}, \tag{1}$$

$$p(x) = \sum_{i=1}^{4} p(x|c_i)p(c_i)$$

where x is the feature vector, $p(x|c_i)$ and $p(c_i)$ are the conditional and prior probabilities, respectively. We are assuming that the features are independent and have a Gaussian distribution, therefore, $p(x|c_i)$ can be calculated as

$$p(x|c_i) = \frac{1}{(2\pi)^{d/2}|\sum_i|^{1/2}} \exp[-1/2(x-\mu_i)^t \times \sum^{-1}(x-\mu_i)], \quad (2)$$

where μ_i is the mean, $\sum_i$ is the covariance matrix. Assuming $p(c_i)$, $i = 1, 2, 3, 4$, are equal, an image can be classified to the class with the maximum conditional probability, i.e., Maximum Likelihood classification.

2.2. Image segmentation

The goal of our segmentation method is to segment the teeth from the background, in bitewing images, and extract for each tooth the contour of the crown and the root. Since dental radiographs often suffer from poor quality, low contrast and uneven exposure that complicate the task of segmentation, the segmentation is the most challenging step in the whole system, and could critically affects the accuracy of the system.

Our proposed segmentation method consists of three steps, region of interest (ROI) localization, image enhancement, and tooth segmentation. The ROI localization step isolates the region of each tooth from the image. The image enhancement step is performed before segmentation to improve the quality of the dental X-ray images. The tooth segmentation step obtains the contour of each tooth and separates it into crown and root parts with the help of bones information.

2.2.1. ROI localization

If we can separate the image into ROI regions, where each region contains only one tooth, it will then become easier to segment the tooth from the background. We use the method of active contours, i.e., "snakes", to separate the ROI regions.

A traditional snake is a curve, $v(s) = [x(s), y(s)]$, $s \in [0, 1]$, that moves through the spatial domain of an image to minimize an energy function given by

$$E = \int_0^1 \left[\frac{1}{2}(\alpha|v'(s)|^2 + \beta|v''(s)|^2) + E_{ext}v(s)\right] ds \quad (3)$$

where α and β are weighting parameters that control the snake's tension and rigidity, respectively, and $v'(s)$, $v''(s)$ denote the first and second derivatives of $v(s)$ with respect to s. The external energy function E_{ext} is derived from the image so that it will have small values at the features of interest [16]. In our work, we use the external energy function defined by

$$E_{ext}(x, y) = G_\sigma(x, y) * I(x, y) \quad (4)$$

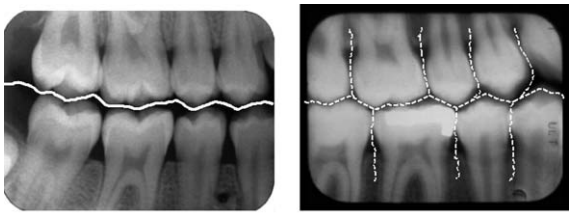

(a) (b)

Fig. 5. ROI localization using snakes (a) separation of upper and lower teeth; (b) separation of individual tooth.

where $I(x, y)$ is the gray-level image, and the G_σ(x) is a two-dimensional Gaussian function with standard deviation σ. With this definition, the function E_{ext} will have smaller values at bones and background areas that separate individual teeth. A large σ will cause the image to blur, which is often necessary to increase the capture range of the active contour.

Fig. 5a shows the result of separating the upper and the lower jaws in a bitewing image using this algorithm. The white line is the result from the "snakes" method after several iterations on the initial line, where the initial line is horizontal or near horizontal and runs across the middle part of the image through the area of the lowest intensity. The initial line is obtained using horizontal integral projection [17,15]. With the assumption that there exists a horizontal or near horizontal straight line with an angle θ that could be used as an approximation for separating the upper and the lower jaws, the integral projection function, defined in Eq. (5), will have the minimal value at the position of that line:

$$L(\theta, x) = \sum_y I^\theta(x, y) \quad (5)$$

where the I^θ is the original image rotated by θ. x and θ together determine the initial near horizontal line for the snakes method. To separate the teeth in each jaw, the initial separating lines are obtained using vertical integral projection. Fig. 5b shows one example of separating teeth using the "snakes" method.

In dental image segmentation, identifying missing teeth is a very important issue. Once the missing teeth are identified in the image at the ROI localization stage, this information can help in the matching stage. For example, if a PM image contains teeth in positions corresponding to missing teeth in an AM image, this means a match is impossible.

We developed a method to identify missing teeth areas after locating the initial lines which separate the teeth in each jaw using integral projection. Fig. 6a shows a bitewing image with a molar tooth missing. Fig. 6b shows the lines obtained by integral projection, where each separated region contains only one tooth. The middle vertical line actually runs across a missing tooth region. To identify a missing tooth, we first use region growing to obtain the dark area

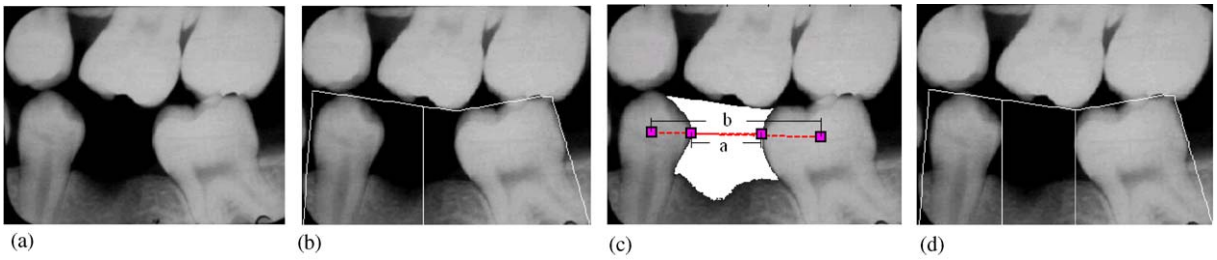

Fig. 6. Missing tooth detection (a) original image; (b) initial localization result from integral projection; (c) features for detection of a missing tooth; (d) final result.

around the initial line, which corresponds to the missing tooth or air, and calculate the centers of mass for the two adjacent regions (surrounding teeth), shown as Fig. 6c. Let b be the distance between the two centers of mass, and a be the portion of b that lies inside the dark region. Assuming that the dark area is either a missing tooth or a gap between teeth, to decide which class the area belongs to, we use the ratio of a to b as the feature and apply a Bayes classifier to classify it based on this feature. The Bayes classifier is designed using the following decision functions:

$$d_j(x) = p(x|w_j)p(w_j) \quad j = 1, 2, \tag{6}$$

where x is the ratio of a to b, w_1 denotes the missing tooth class, and w_2 denotes the gap class. $p(w_j)$ and $p(x|w_j)$ are the prior and conditional probability distributions for class w_j. We estimated the conditional probability distributions of the two classes from a training set of 26 images, where half of them have a missing tooth.

A dark area with a feature value x is assigned to missing tooth class if $d_1(x)$ is greater than $d_2(x)$. If the dark region is for a missing tooth as in Fig. 6b, the middle vertical line has to be replaced by two new lines closer to the adjacent teeth, shown as Fig. 6d.

2.2.2. Enhancement

Dental radiographs often suffer from low contrast and uneven exposure that complicate the task of segmentation. Applying enhancement usually helps the segmentation. Dental radiographs have three distinctive regions: background (the air), teeth, and bones (see Fig. 7). Usually the teeth regions have the highest intensity, the bone regions have high intensity that sometimes is close to that of the teeth, and the background has a distinctively low intensity. Threshold can be used to separate the background from the image, but threshold methods may fail to discriminate teeth from bones because their intensities are sometimes similar, especially in cases of uneven exposure. In order to prepare the image for successful segmentation, the first step is to enhance the image's contrast by making the teeth regions brighter and suppressing the intensity in the bone and the background regions.

Fig. 7. A typical dental X-ray image.

Two morphological filters, top-hat filter and bottom-hat filter, can be used to extract light objects (or, conversely, dark ones) on a dark (or light) but slowly changing background [18,19]. The top-hat filter returns the difference between the result of morphological opening operation and the original image. The bottom-hat filter is performed by subtracting the original image from the result of grayscale closing operation. To enhance the bright regions that correspond to the teeth, top-hat filter is applied using a structure element, whose size corresponds to the radius of the largest intensity peak that can be detected. Similarly, to enhance the dark bones and air areas, bottom-hat filter is applied to produce large pixel values in the result, where there are small dark regions in the original image.

In our method, we use both top-hat and bottom-hat filtering operations on the original image. The enhanced image is obtained by adding to the original image the result of the top-hat filter and subtracting the result of the bottom-hat filter, as follows:

$$\begin{aligned}\text{EnhancedImage} = \text{OriginalImage} + \text{top-hat}(\text{OriginalImage}) \\ - \text{bottom-hat}(\text{OriginalImage}).\end{aligned} \tag{7}$$

Fig. 8 shows an example of applying the above enhancement algorithm on a bitewing dental image. Fig. 8a shows the original image and Figs. 8b and c show the results of applying the top-hat and the bottom-hat filters, respectively. Fig. 8d shows the resulting enhanced image, where the teeth have been brightened and the background and the bone regions have been suppressed.

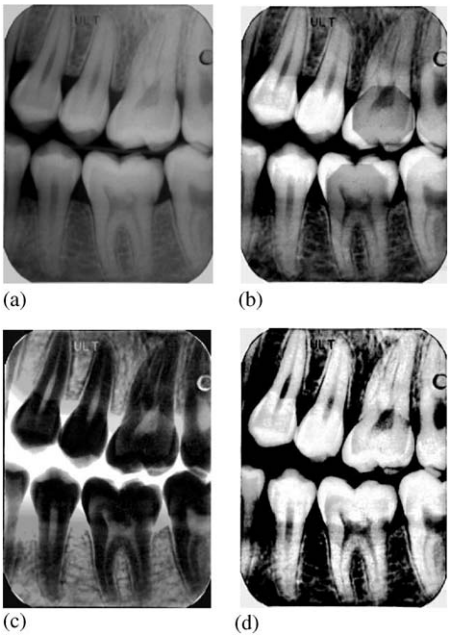

Fig. 8. An example of dental image enhancement: (a) original image; (b) result of top-hat filtering; (c) result of bottom-hat filtering; (d) the final enhancement result.

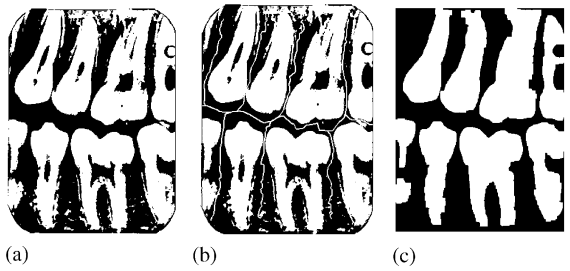

Fig. 9. An example of teeth segmentation: (a) result of adaptive thresholding; (b) teeth regions isolation using the result from ROI localization; (c) result after morphological operations.

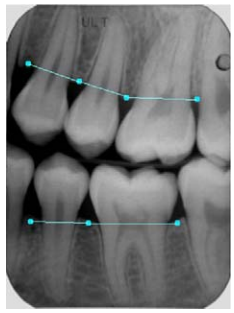

Fig. 10. Separation of crowns and roots.

2.2.3. Teeth segmentation

After obtaining the enhanced image using top-hat and bottom-hat filters, the system segments the images as follows. First, it obtains the initial contours. Then it refines these initial teeth contours using the active contour method. Finally, the teeth contours are separated into the crowns and the roots.

A window-based adaptive threshold is used to segment the enhanced image to minimize the influence of uneven intensity and noise in the bone regions [20]. The idea of window-based adaptive threshold is to examine the intensity values of the local neighborhood of each pixel. If the intensity value of the pixel is larger than the average intensity of its neighbors, then it is classified as belonging to a tooth, otherwise it is classified as belonging to background. Next, the system uses the results from ROI localization to isolate each tooth region in the threshold image. Then, it applies size filtering to smooth the teeth region and remove noisy areas [21–23]. The initial teeth contours are extracted from the teeth regions in the images.

Due to the variations in the quality of dental images, sometimes the initial contours are not good enough to ensure successful matching. To overcome this problem, we apply the "snakes" method again to refine the contours and obtain more reliable results. Here the external energy function is different from the one used for ROI localization. The external energy function is a Laplacian of Gaussian operation as defined in Eq. (8), and it will have small values at step edges and will lead the snake towards boundaries of teeth [24]:

$$E_{ext} = -|\nabla[G_\sigma(x, y) * I(x, y)]|^2. \quad (8)$$

Fig. 9 shows an example of the teeth segmentation stage for the image whose enhancement result was shown in Fig. 8. Fig. 9a is the segmented image using the window-based adaptive threshold. Fig. 9b shows the isolated teeth regions using the results from ROI localization. Fig. 9c shows the separated and smoothed teeth regions that are used for extracting initial teeth contours.

After obtaining the final teeth contours from the active contours, the system will separate them into crown and root parts. Basically, the crown is the upper part of the tooth outside the gum, and the root is the part of the tooth that sits in bones between teeth. Positions of the bones provide important information to separate the crown and the root parts of the teeth. As shown in Fig. 10, lines that connect the tips of the bones approximate the gum line, which separate teeth into crowns and roots.

To obtain the positions of the tips of the bones, the system segments the bones from the original image. This is achieved by subtracting the segmented teeth from the original image followed by a threshold operation to segment the bones from the background (see Fig. 11).

In a bitewing dental image (see Fig. 10), there are two gum lines, the upper jaw's gum line and the lower jaw's

Fig. 11. Segmented bones image.

gum line, that need to be located. To do this, the system first splits the bones image into two parts, one contains lower jaw's bones and the other contains upper jaw's bones. The split is done by using the result from ROI localization. In these images, the bones are usually not vertical, but have a slope with the vertical direction. To determine the slope of the bones in each jaw, the system rotates the image in a range of angles, e.g., $[-30, 30]$, with an interval of 1°, and establishes a vertical integral projection for each rotated image:

$$H^{\theta}(y) = \sum_{x} B^{\theta}(x, y), \tag{9}$$

where $B^{\theta}(x, y)$ is the rotated bones image, and θ denotes the angle of rotation. The rotation angle β that makes the bones vertical will result in many zero values in $H^{\beta}(y)$, and therefore the standard deviation of $H^{\beta}(y)$, as calculated in Eq. (10), will most probably have the maximum standard deviation value among all $Std(H^{\theta}(y))$, $\theta \in [-30, 30]$:

$$Std(H^{\theta}) = \left[\frac{1}{M-1} \sum_{y=1}^{M} (H^{\theta}(y) - \bar{H}^{\theta})^2 \right]^{1/2}, \tag{10}$$

where M is width of the bones image and

$$\bar{H}^{\theta} = \frac{1}{M} \sum_{y=1}^{M} H^{\theta}(y). \tag{11}$$

Thus the slope of bones can be determined as β. Fig. 12 shows an example of the vertical integral projection. The upper row of Fig. 12 shows the original bone image of the upper jaw and the rotated version of the image, where the bones are almost vertical. The lower row of the figure shows their integral projections, where it is clear that the second image produces more zero values as evident by the larger intervals of zeros.

When the bones are vertical in a rotated image, the tips can be easily localized. The positions in the original image can be computed according to the rotation angle between the rotated image and the original image. Finally, by connecting these tips in the original image and locating the intersection points with teeth contours, the teeth contours are separated into roots and crowns (see Fig. 13). Two examples of segmentation with crowns and roots separated are shown in Fig. 14.

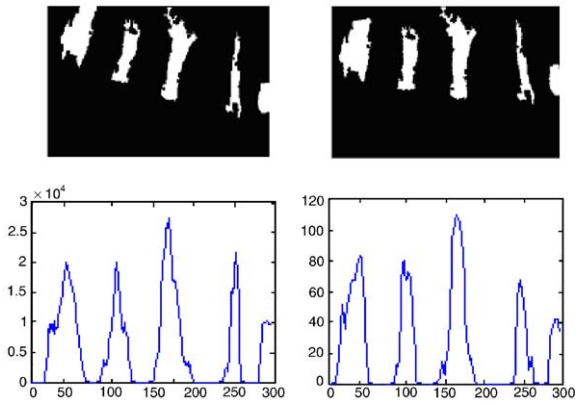

Fig. 12. Bone image and its rotated version with the integral projection for both images.

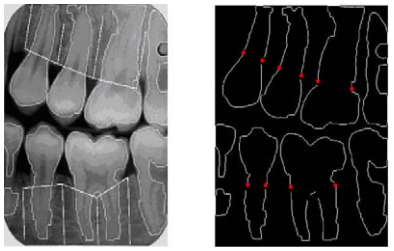

Fig. 13. Separated roots and crowns.

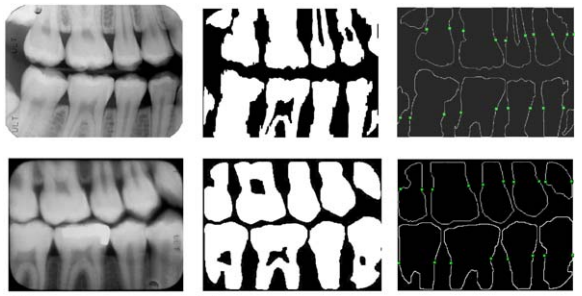

Fig. 14. Teeth segmentation and separation of crowns and roots: (a) original images; (b) results of adaptive thresholding; (c) refined teeth contours with points that separate the roots and crowns.

2.3. Shape-based retrieval

The extracted contours are used in calculating the distance between the submitted PM case and the cases in the

Fig. 15. Sample of the Images used in dental image classification.

AM database. Sometimes the teeth in the dental images are partially visible. Therefore, the extracted boundaries in these images can be partial boundaries of the teeth. This can happen for both AM and PM teeth. To solve this problem, we apply partial bi-directional Hausdorff distance [25] for shape matching.

The partial bidirectional Hausdorff distance as a function of an affine transformation (i.e., rotation, scale and translation) of the PM shape, and the AM shape is defined as

$$H_{LK}(T(P), P') = \max(h_L(P', T(P), h_K(T(P), P'))), \tag{12}$$

where P is the PM tooth boundary, T(P) is the transformation of P, which can be represented as

$$T(P) = A * P + t = \begin{pmatrix} \cos\theta, & \sin\theta \\ -\sin\theta, & \cos\theta \end{pmatrix} * \begin{pmatrix} s & 0 \\ 0 & s \end{pmatrix} * \begin{pmatrix} x \\ y \end{pmatrix} + \begin{pmatrix} t_x \\ t_y \end{pmatrix}, \tag{13}$$

where P' is the boundary of the AM tooth, $h_k(T(P), P')$ is the partial directed distance from $T(P)$ to P', where $1 \leqslant K \leqslant q$ (q is the number of points of P), and $h_L(P', T(P))$ is the partial directed distance from P' to $T(P)$, $1 \leqslant L \leqslant q'$ (q' is the number of points of P'). The definition of partial directed distance, e.g., $h_k(T(P), P')$ denotes the Kth ranked value in the set of distances from $T(P)$ to P'. That is, for each point of $T(P)$, the distance to the closest point of P' is computed, and then the points of $T(P)$ are ranked based on the respective distances. The Kth ranked distance value tells us that K of the points $T(P)$ are each within that distance of some points in p'. This process automatically selects the K best matching points in $T(P)$, which means that matching only takes a portion of the contour points into consideration. In practice, to compute the partial directed distance, we specify some fractions f_1, f_2, where $0 < f_1, f_2 < 1$, and let $K = f_1 * q$, $L = f_2 * q'$. The fractions f_1, f_2 determine how much missing points of the AM and PM teeth contours we can tolerate.

The matching is performed by finding a transformation (i.e., rotation, scale and translation), that results in a minimum Hausdorff distance. As mentioned earlier in the paper, our segmentation method can separate each tooth into crown and root, matching starts by establishing initial correspondence between boundary points to limit the search space and efficiently calculate the Haustorff distance. Since the crowns are usually visible, the system can align the two boundaries using only the points of the crowns to obtain the initial parameters of the transformation. Then the minimum Hausdorff distance is found using Quadratic Programming optimization method [26].

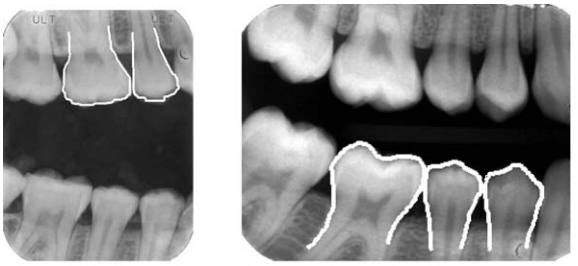

(a) (b)

Fig. 16. Query teeth shapes from PM images: (a) a molar together with an adjacent premolar; (b) one molar together with two premolars.

For each query shape and a database shape pair, the shape distance is defined as the minimized Hausdorff distance normalized by the scaling factor s used in Eq. (13). Finally, the system ranks the shape distances of AM images to generate a list to present to the user. The AM image that has minimum Hausdorff distance to the PM image is considered as the best match.

3. Experimental results

In the dental image classification experiment, we used 60 images as the training set, with 15 images obtained from each of the four types of dental images, e.g. panoramic, bitewing, lower periapical and upper periapical images. The proposed image classification algorithm was tested on a set of 123 images, in which 9 are panoramic images, 82 are bitewing images, 15 are lower periapical images and 17 are upper periapical images. Fig. 15 shows few of the images that we used in the experiments. In our classification experiments, 5 cases were misclassified out of 123 cases, i.e., the error rate was 4%.

We also evaluated the overall performance of the system for retrieval. We used a set of 102 bitewing AM images in our experiment. The contours of the teeth in these AM images were extracted and archived in the AM database. To enhance the chances of correct identification, we used for queries two or three adjacent molar and pre-molar teeth together. Fig. 16 shows two typical query shapes from PM images. By using the contours of several teeth simultaneously rather than single tooth, more information such as the relative positions and the distances between teeth is utilized, which help produce more robust retrieval results.

We tested the algorithm for retrieval using 40 PM images. Since the relative positions of teeth in different jaws may change due to the movement of the jaws, we divide the teeth in the dental image into two groups: the upper jaw teeth and the lower jaw teeth. For each PM image, two queries corresponding to the upper and the lower jaws were formed. The final matching distance between the PM image and the AM image takes into account the retrieval results from the two queries. This is achieved by using the average matching distances of the two queries as the matching distance between the PM image and an AM image. The AM image that has the minimum matching distance is considered the most similar image to the PM image. Given a PM image the system retrieves the most similar AM images in the database using the bidirectional Hausdorff matching distance.

Fig. 17 shows an example, where both the two queries from the PM image obtain the correct AM image as the first match. Fig. 18 shows another example, where the query from upper jaw of the PM image obtains the correct AM image as the best match, whereas the query from the lower jaw obtains the correct AM image as the second match. The final result after using the average matching distance gives the correct AM image as the best match.

Among the 40 submitted PM images, 33 out of the 40 images obtained the correct AM images as the most similar images. For the remaining seven images, three of them obtained the correct AM images as the second most similar images; the other four images obtained the correct AM images as the 3rd, 4th, 7th, and 11th most similar images. This means that if the user looks only at the top five most similar images, the system has a precision of 95%. The reasons for the cases where the correct AM images do not rank first could be (1) the teeth shapes extracted from AM images are not very accurate because of the image quality, (2) the shape of the same tooth in AM and PM images may vary due to changes in the viewing angle, and (3) tooth shape may vary because of aging.

4. Conclusion and future work

In this paper we presented a content-based archiving and retrieval system of dental images for use in human identification. It contains three major stages: dental image classification, bitewing image segmentation and retrieval based on teeth shapes using bidirectional Hausdorff distance. In the classification stage, two features are proposed for dental X-ray image classification. The classified bitewing images are segmented to extract the contours of molars and premolars, which are then used to archive the images in an AM database. During retrieval, a PM bitewing image is segmented to extract teeth contours, which are used to find the most similar images in the AM database using Hausdorff distance measure. The experiments show that the three stages of the system are robust. Most of the images that we have could be well segmented. For the case where there is overlap between the teeth, more work needs to be done for the segmentation step.

Our future work will focus on using more features for image retrieval in addition to geometry-based features, and developing algorithms to allow fast retrieval. We will also work on extending the segmentation algorithm to handle the

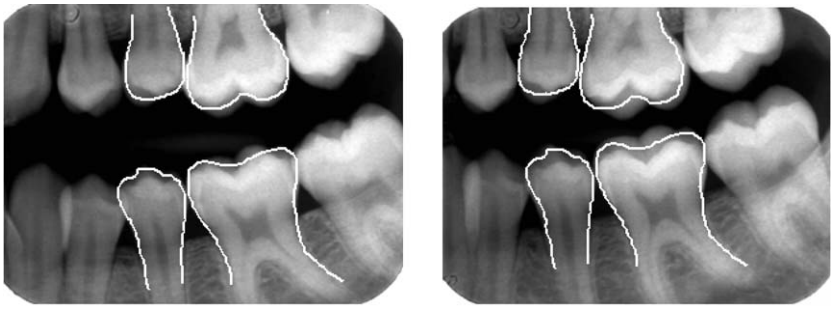

Fig. 17. Both query teeth shapes get the correct AM image as the first match. (a) PM image with query shapes and (b) correct AM image with the query shapes. Matching distance is 6.9096.

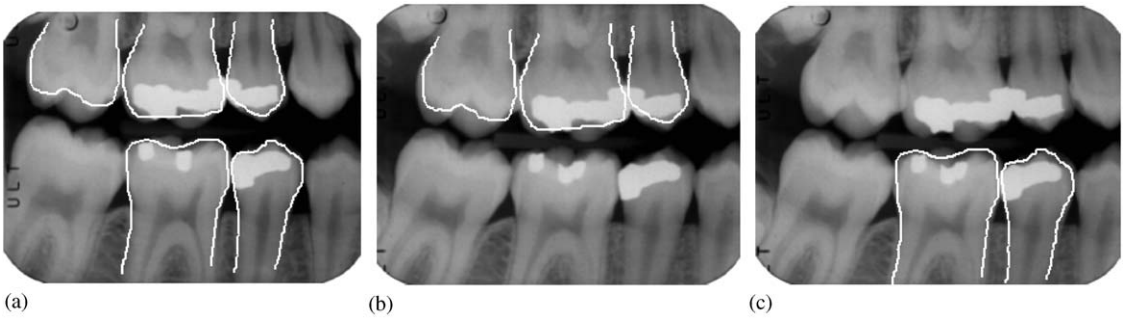

Fig. 18. (a) PM image with query shapes. (b) Upper jaw query superimposed on the correct AM image that was retrieved as the best similar image. (c) Lower jaw query superimposed on the correct AM image that was retrieved as the second most similar image. Final matching distance was 11.1521 for the correct image.

image with poor quality and to segment the other two types of dental images, i.e., panoramic and periapical.

References

[1] F.S. Malkowski, Forensic dentistry, a study of personal identification, Dent. Stud. 51 (1972) 42–44.
[2] V.W. Weedn, Postmortem identifications of remains, Clin. Lab. Med. 18 (1998) 115–137.
[3] R.B. Dorion, Disasters big and small, J. Can. Dent. Assoc. 56 (1990) 593–598.
[4] I.A. Pretty, D. Sweet, A look at forensic dentistry—Part 1: The role of teeth in the determination of human identity, Br. Dent. J. 190 (7) (2001) 359–366.
[5] American Society of Forensic Odontology, Forensic Odontology News, vol. 16, no. 2, Summer 1997.
[6] United States Army Institute of Dental Research Walter Reed Army Medical Center, Computer assisted post mortem identification via dental and other characteristics, USAIDR Inf. Bull. 5(1) (1990).
[7] Dr. Jim McGivney et al., WinID2 software (www.winid.com).
[8] Jonasson, Bankvall, Kiliaridis, Estimation of skeletal bone mineral density by mean of the trabecular pattern of the alveolar bone, its interdental thickness, and the bone mass of the mandible, Oral Surg. Oral Med. Oral Pathol. 92 (2001).
[9] The Canadian Dental Association, Communique, May/June 1997.
[10] P. Stimson, C. Mertz, Forensic Dentistry, CRC Press, Boca Raton, FL, 1997.
[11] Gustafson, Ghosta, Forensic Odontology, American Elsevier Pub. Co., 1996.
[12] A. Jain, L. Hong, S. Pankanti, Biometric identification, Commun. ACM 43 (2) (2000) 91–98.
[13] S. Pankanti, R. Bolle, A. Jain, Biometrics: the future of identification, IEEE Comput. (2000) 46–49.
[14] A.K. Jain, H. Chen, S. Minut, Dental biometrics: human identification using dental radiographs, Proceedings of the AVBPA 2003, Fourth International Conference on Audio- and Video-Based Biometric Person Authentication, Guildford, UK, June 2003, pp. 429–437.
[15] M. Abdel-Mottaleb, O. Nomir, D. Eldin Nassar, G. Fahmy, H. Ammar, Challenges of Developing an Automated Dental Identification System, IEEE Mid-west Symposium for Circuits and Systems, Cairo, Egypt, December 2003.
[16] C. Xu, J.L. Prince, Snakes, shapes, and gradient vector flow, IEEE Trans. Image Process. 7 (3) (1998) 359–369.

[17] R. Brunelli, T. Poggio, Face recognition: features versus templates, IEEE Trans. PAMI 15 (10) (1993) 1042–1052.
[18] M. Sonka, V. Hlavac, R. Boyle, Image Processing, Analysis, and Machine Vision, second ed., Thomson, 2001.
[19] L. Vincent, Morphological grayscale reconstruction in image analysis: application and efficient algorithms, IEEE Trans. Image Process. 2 (2) (1993) 176–201.
[20] J.R. Parker, Algorithms for Image Processing and Computer Vision, Wiley, New York, 1996.
[21] S. Hu, E.A. Huffman, Automatic lung segmentation for accurate quantitation of volumetric X-ray CT images, IEEE Trans. Med. Image 20 (6) (2001) 490–498.
[22] C. Giardina, E. Dougherty, Morphological Methods in Image and Signal Processing, Prentice-Hall, Englewood Cliffs, NJ, 1988.
[23] H.J.A.M. Heijmans, Morphological Image Operators, Academic Press, Boston, 1994.
[24] H. Park, T. Schoepflin, Y. Kim, Active contour model with gradient directional information: directional sanke, IEEE Trans. Circuits Systems Video Technol. Digital Image Process. 11 (1) (2001) 252–256.
[25] D.P. Huttenlocher, G.A. Klanderman, W.J. Rucklidge, Comparing images using the Hausdorff distance, IEEE Trans. PAMI 15 (9) (1993) 850–863.
[26] S.P. Han, A globally convergent method for nonlinear programming, J. Optim. Theory Appl. 22 (1977) 297.
[27] A.K. Jain, H. Chen, Matching of Dental X-ray Images for Human Identification, Pattern Recognition, pp. 1519-1532, July 2004.
[28] J.D. Zhou, M. Abed-Mottaleb, Automatic human identification based on dental X-ray images, Proceedings of the SPIE Conference on Defense and Security, Biometric Technology for Human Identification, 2004.

About the Author.—JINDAN ZHOU received the B.S. and M.S. degrees in Biomedical Engineering from Southeast University, Nanjing, China, in 1999 and 2002. She is now a Ph.D. student at the Department of Electric and Computer Engineering, University of Miami, Coral Gables, FL, USA. Her current research interests include image processing, pattern recognition and biometrics.

About the Author—MOHAMED ABDEL-MOTTALEB received his Ph.D. in computer science from University of Maryland, College Park, in 1993. He is an associate professor in the department of Electrical and Computer Engineering, University of Miami, where his research focuses on 3D face recognition, dental biometrics, visual tracking, and human activity recognition. Prior to joining the University of Miami, from 1993 to 2000, he worked at Philips Research, Briarcliff Manor, NY. At Philips Research, he was a Principal Member of Research Staff and a Project Leader, where he led several projects in image processing, and content-based multimedia retrieval. He holds 20 US patents and published over 60 papers in the areas of image processing, computer vision, and content based retrieval. He is an associate editor for the Pattern Recognition journal.